





Article

Spatial Structure and Temporal Dynamics in Clear Lake, CA: The Role of Wind in Promoting and Sustaining Harmful Cyanobacterial Blooms

David A. Caron ^{1,*} , Alle A. Y. Lie ² , Brittany Stewart ¹ , Amanda Tinoco ¹, Isha Kalra ¹, Stephanie A. Smith ³, Adam L. Willingham ⁴, Shawn Sneddon ⁵, Jayme Smith ² , Eric Webb ¹, Kyra Florea ¹ and Meredith D. A. Howard ⁶

¹ Department of Biological Sciences, University of Southern California, 3616 Trousdale Parkway, Los Angeles, CA 90089, USA; bs70959@usc.edu (B.S.); ishakalr@usc.edu (I.K.)

² Southern California Coastal Water Research Project, Costa Mesa, CA 92626, USA; allel@sccwrp.org (A.A.Y.L.); jaymes@sccwrp.org (J.S.)

³ In-Situ Environmental, Fort Collins, CO 80524, USA

⁴ Badger Meter, Seaside, CA 93955, USA

⁵ Xylem Water Solutions, Washington, DC 20003, USA; shawn.sneddon@xylem.com

⁶ Sacramento-San Joaquin Delta Conservancy, 1450 Halyard Drive, Suite 6, West Sacramento, CA 95691, USA; meredith.howard@deltaconservancy.ca.gov

* Correspondence: dcaron@usc.edu; Tel.: +1-213-740-0203

Abstract

Clear Lake in Lake County, CA, USA has experienced highly toxic cyanobacterial blooms for more than a decade, with multiple cyanobacterial taxa and cyanotoxins appearing sporadically, typically throughout much of the early-spring to late-fall seasons. Recurring blooms have been attributed to high internal nutrient loads within the lake, with hydrography and hydrology playing important but still poorly documented roles in controlling the availability of growth-limiting elements to the phytoplankton community. The lake is approximately 180 km² in areal extent and composed of three somewhat disjointed lobes, or ‘Arms’. The large size of the lake presents a formidable task for synoptic lakewide surveys and for understanding the specific features that stimulate the development and magnitude of harmful blooms. We conducted a study in August of 2020 that involved the use of an autonomous underwater vehicle and deployment of a hand-held water column profiler to describe the lakewide status of various biological, chemical, and physical features. Discrete water samples were also collected from ten stations located throughout the lake to produce a near-synoptic depiction of lake status. Additionally, a mechanically driven, continuously monitoring water-column profiler was deployed at a central lake location to document short-term temporal (minutes to months) changes in water-column structure and chemistry. Wind was a dominant feature affecting the lake’s chemistry and biology during the study, resulting in massive concentrations and dramatic spatial heterogeneity of phytoplankton biomass and cyanotoxins in the eastern and southeastern Arms of the lake, and confirmed by the analysis of discrete water samples. Unique insight into the processes leading to or prolonging blooms was revealed by the water column profiler, which demonstrated rapid development (within a few hours) of suboxic conditions during periods of calm winds. We speculate that these quiescent periods are fundamental events in the lake’s ecology, resulting in episodic ‘pulses’ of nutrient release from the sediments, which can stimulate or refuel blooms of cyanobacteria in the water column.

Keywords: harmful algal blooms; water column structure; nutrients; anoxia



Academic Editor: Yuanrong Zhu

Received: 28 September 2025

Revised: 4 November 2025

Accepted: 12 November 2025

Published: 15 November 2025

Citation: Caron, D.A.; Lie, A.A.Y.; Stewart, B.; Tinoco, A.; Kalra, I.; Smith, S.A.; Willingham, A.L.; Sneddon, S.; Smith, J.; Webb, E.; et al. Spatial Structure and Temporal Dynamics in Clear Lake, CA: The Role of Wind in Promoting and Sustaining Harmful Cyanobacterial Blooms. *Water* **2025**, *17*, 3265. <https://doi.org/10.3390/w17223265>

Copyright: © 2025 by the authors. Licensee MDPI, Basel, Switzerland. This article is an open access article distributed under the terms and conditions of the Creative Commons Attribution (CC BY) license (<https://creativecommons.org/licenses/by/4.0/>).

1. Introduction

Clear Lake in Lake County, California, USA, is the oldest natural lake completely within the state of California. The lake has a surface area of approximately 180 km², composed of three interconnected lobes, or 'Arms', and is relatively shallow (average depth \approx 10 m). The long axis of the lake (\approx 30 km) is oriented such that the lake experiences a long wind fetch in the prevailing wind direction. As a consequence, the lake is strongly affected by wind stress and is polymictic. Clear Lake has witnessed human occupation and influence for more than 10,000 years. Analyses of sediment cores have indicated that it has been eutrophic at least since the end of the Pleistocene [1], but a history of activities (e.g., damming, mercury mining) and land uses has strongly impacted the lake's ecology and environmental condition within the last few centuries [1–3].

The three Arms of Clear Lake could be described as a collection of meta-ecosystems [4] given the high degree of biological variability among them. The metacommunities occupying these disparate regions of the lake overlap, but they can also constitute somewhat distinct entities with different food web structure and dynamics [5]. There is also considerable horizontal and vertical spatial variability within each of the Arms. These features are problematic when, as in the present study, the goal is to assess the overall distribution and abundance of phytoplankton biomass and associated water chemistry throughout the lake.

Clear Lake is presently hypereutrophic, with high rates of primary production having been documented for at least 60 years [6]. Cyanobacteria have been a significant component of the phytoplankton community in the lake for decades, often exhibiting highly heterogeneous spatial distributions at the surface of the lake [7]. Particularly high cell abundances of several cyanobacteria accompanied by high chlorophyll concentrations have been observed in the lake within the last few decades, including *Anabaena*, *Microcystis*, *Dolichospermum*, *Gloeotrichia*, *Aphanizomenon*, *Lyngbya*, and others [8]. In particular, *Microcystis* has been a recurring bloom-former and putative toxin-producing cyanobacterium in Clear Lake during recent years. Repeated high levels of cyanotoxins in the lake, and in some cases in drinking water derived from the lake, have focused public attention on the health risks posed by these toxic cyanobacterial harmful algal blooms (cHABs) [9,10].

The sources of nutrients promoting cHABs and toxin production in Clear Lake have been topics of intense research since highly toxic conditions were demonstrated more than a decade ago [11]. Reviews of historical data have pointed to the importance of internal nutrient loads, and, in particular, very large amounts of phosphorus in the sediments of the lake, as a leading cause of recurrent blooms and toxic conditions [3,8]. A 2019–2021 study to quantify external and internal nutrient loading for Clear Lake concluded that internal sources of phosphorus accounted for most of the phosphorus driving blooms in the lake [12]. As a consequence, phosphorus has become a regulatory target to reduce the high nutrient concentrations driving blooms. A Total Daily Maximum Load (TMDL) was established for phosphorus in 2007 in an effort to reduce external loading of this essential element [13]. Despite the imposition of the phosphorus TMDL, however, highly toxic blooms continue to occur in the lake.

A historical review supporting an important role for anoxia and the consequent phosphorus release from the sediments of Clear Lake (i.e., internal phosphorus loading) has recently been published [14]. The authors noted a correlation between anoxia and hypolimnetic soluble reactive phosphorus and total phosphorus concentrations over multi-decadal time scales. A link between the general timing and duration of anoxia in the lake and the appearance of cyanobacterial blooms also implicates internal phosphorus loading as a driver of cHABs during the summer in Clear Lake [12]. In the latter study, the timing of blooms did not correlate with spring runoff events, which constitute a substantial portion

of the lake's external nutrient loading, further implicating internal loading as a major driver of blooms.

Recognition of the importance of internal phosphorus loads as a causative factor in Clear Lake's toxic cyanobacterial blooms has also raised attention regarding the role that wind plays in affecting lake chemistry and biology. Wind has long been recognized as a strong influence on water column structure and the spatial distribution and dynamics of phytoplankton in lakes [15]. The orientation of the long axis of Clear Lake from northwest to southeast, in line with the prevailing northwesterly wind, creates an extensive fetch (approximately 30 km) and results in well-known, highly heterogeneous spatial distributions of phytoplankton in the lake [8]. Unfortunately, quantitatively characterizing that heterogeneity and consequent changes in lake chemistry and physics are difficult because of the lake's large size.

Wind also strongly affects vertical water movement locally within the lake, influencing the vertical mixing of dissolved oxygen concentrations into deep waters, which in turn affects phosphorus release from sediments due to changing redox conditions. Significant periods of calm winds can lead to oxygen depletion in hypereutrophic Clear Lake, whereas sustained winds would be expected to result in water-column turnover and oxygen replenishment to the deep waters of this polymictic lake. Previous studies have measured and modeled wind-induced, basin-scale circulation in the lake [16–18], yet understanding how these circulation patterns change over short time periods, and their consequent impact on nutrient cycling, has been difficult.

Automated sensing approaches have begun to address the difficulties associated with assessing overall water quality in large waterbodies and their responsiveness to changing environmental conditions. Such approaches are now providing unique insights into the spatial distributions of phytoplankton populations [19–21] and short-term changes in water column structure that affect biology [22–25].

The objective of this study was to characterize the horizontal and vertical spatial heterogeneity of phytoplankton biomass and several biologically relevant chemical parameters on time scales relevant to the initiation or prolongation of cHABs in Clear Lake during August 2020. The spatial distribution of chemical and biological parameters across the expanse of the lake was documented using an autonomous underwater vehicle, augmented by assessing water column structure using a handheld sensor package and the analysis of discrete water samples at stations located throughout the lake. Additionally, high-frequency temporal data of water column chemistry were obtained using a mechanically driven, continuously monitoring water column profiler. Phytoplankton distribution and biologically mediated chemical parameters were highly heterogeneous across the long axis of Clear Lake during the study, with massive accumulations in the eastern and southeastern portions of the lake. Wind-driven mixing of the water column dominated most of the study period, but short intervals of calm winds resulted in the rapid (within hours) onset of hypoxic conditions in the deeper waters of the lake. We speculate that these brief periods of calm winds, resulting in short periods of anoxic bottom waters and presumed redox-controlled phosphorus release from sediments, may be fundamental but previously overlooked processes leading to bloom stimulation or prolongation.

2. Materials and Methods

Several modes of sensing and sampling were conducted in Clear Lake, Lake County, California, USA during August 2020 (Figure 1A,D). An autonomous underwater vehicle (AUV) was employed in transects along the main axes of the lake conducted over a 3-day period to gather a single, near-synoptic picture of water-column structure and chemistry (temperature, chlorophyll-*a* fluorescence, dissolved oxygen concentration) across the entire

lake. The AUV mission was complemented with boat surveys conducted eight times at ten stations throughout August to collect discrete near-surface water samples for measurements of extracted chlorophyll-*a*, cyanotoxin concentrations (microcystins), total nitrogen, and total phosphorus concentrations. Water column characterizations (temperature and dissolved oxygen concentrations with depth) were also performed at each station on all dates using a handheld sensor package. Finally, high-temporal frequency measurements (temperature, dissolved oxygen, chlorophyll-*a* fluorescence) of water column structure were obtained for nearly the entire month at a single station using a mechanically driven profiling instrument package.

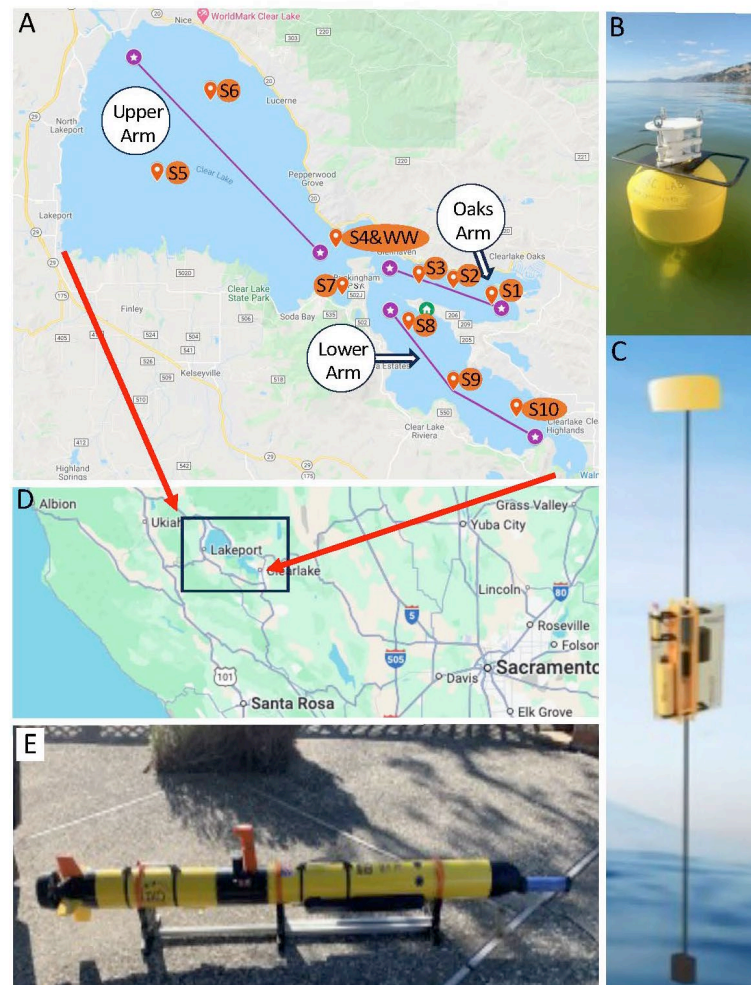


Figure 1. Major instrumentation and map of the study area in Clear Lake, Lake County, California. A map of the lake (A) and its regional location in northwestern California, USA (D) ((A,D) images from Google Maps). Purple lines in (A) indicate approximate mission lines in each Arm of the lake along which the YSI i3XO EcoMapper autonomous vehicle (Xylem, Washington, DC, USA) (E) was deployed, equipped with instruments to measure pertinent chemical/physical parameters. A Wirewalker vertical profiler (Del Mar Oceanographic, San Diego, CA, USA) (B,C) equipped with instruments for continuous measurement of pertinent chemical/physical parameters was deployed at a station near the confluence of the three Arms of the lake (station S4WW in (A)). A hand-held RBR profiling instrument was deployed approximately twice weekly at 10 stations (denoted by ‘S#’ on the map) throughout the lake to obtain vertical profiles of pertinent chemical/physical parameters (A).

2.1. Lakewide Sensing by Autonomous Underwater Vehicle (AUV)

The goal of the AUV missions was to characterize water-column chemistry and biology in Clear Lake as synoptically as possible, given the large size of the lake. A Xylem YSI

i3XO EcoMapper (Figure 1E) was employed to conduct transects along the main axis of each of the lake's three main Arms (Figure 1A). The EcoMapper is a powered AUV that carried sensors that recorded depth, temperature, chlorophyll-*a* fluorescence (a proxy for algal/cyanobacterial biomass), and dissolved oxygen continuously as the instrument moved along a pre-programmed mission line. A total of four transects were conducted along the main axes of Upper Arm (5 August), Oaks Arm (6 August), and two in the Lower Arm (7 August), each of the Lower Arm transects covering approximately half the length of the Arm. The two transects in Lower Arm were combined into a single transect that covered the full length of Lower Arm. A Geo-referenced map of Clear Lake was used to create a mission plan using the software interface VectorMaps® (Xylem, Inc., Washington, DC, USA).

Waypoints were placed at specific locations near the poles of each Arm within the lake (Figure 1A), and the EcoMapper was programmed for autonomous operation. For each mission, the instrument undulated vertically along its horizontal transect line between 1.5 m from the surface (to avoid boat traffic) and 2 m above the lake bottom with a 15-degree dive/rise angle at a speed of 2.5 knots. Initial data analysis was carried out using VectorMaps®. The resulting sensed data were then plotted to provide two-dimensional depictions (horizontal run vs. depth) of each sensed parameter along the transect lines in the lake's Arms (<https://github.com/Jennifer1Beatty/ClearLakeOverview>; URL accessed on 6 June 2025).

2.2. Discrete Water Sample Collections and Water Column Profiling from Boats

Eight surveys were conducted at ten stations (Figure 1A) during 2020 on 5, 8, 11, 14, 18, 21, 25, and 28 August. Approximate station locations are shown in Figure 1A with station coordinates provided in Supplemental Table S1. Whole (i.e., unfiltered) water samples were collected at each sampling location (surface to 0.5 m) using a clean plastic bucket. All collection bottles were acid-cleaned, rinsed with distilled water, and rinsed three times with sample water before filling. Filled bottles were kept cool and in the dark while in the field. Processing of water samples was conducted at an onsite field laboratory within 12 h of sample collection. Water samples were analyzed for nutrients (total phosphorus and total nitrogen), cyanotoxins (microcystins), and extracted chlorophyll-*a* concentration. Net tow samples were preserved with formalin (1% final concentration) for later microscopical analysis to assess community composition and relative abundances. Nutrient, cyanotoxin, and chlorophyll samples were frozen at the field laboratory and stored at -20°C until analyzed.

Water samples analyzed for total nitrogen (TN) and total phosphorus (TP) were collected by aliquoting whole (unfiltered) water into 60 mL HDPE jars. Samples were kept on ice in the field, and frozen at -20°C immediately upon return to the field laboratory. Samples were analyzed colorimetrically following EPA Methods 353.2 for TP and 365.1 for TN at the University of Maryland Center for Environmental Science Nutrient Analytical Services Laboratory.

Water samples analyzed for extracted chlorophyll-*a* consisted of 25 mL of whole (unfiltered) water gently filtered onto glass fiber filters (Sterlitech, grade F, Kent, WA, USA). Filters were extracted in 100% acetone at -20°C for 24 h in the dark. Sample extracts were analyzed fluorometrically via the non-acidification method using a Trilogy Turner Designs fluorometer (Turner Designs, Sunnyvale, CA, USA). Duplicate filters were collected at each station, analyzed separately, and the average chlorophyll *a* concentration of the two filters was reported.

Water samples were analyzed for both total and particulate microcystins. Aliquots (10 mL) of whole (unfiltered) water were frozen for total microcystin analysis, and samples

for particulate microcystin analysis were obtained by filtration onto glass fiber filters, as described for chlorophyll-*a* samples. Both types of samples were lysed via three freeze–thaw cycles to ensure cell disruption, with 3 mL of ultrapure water added to the particulate microcystins sample prior to the freeze–thaw cycles. The extract was then filtered through a 0.2 µm pore-size syringe filter, and extracts for both total and particulate microcystins were analyzed via ADDA ELISA test kits (Abraxis, Part No. 520011, Warminster, PA, USA) according to the manufacturer’s instructions. Samples with concentrations higher than the standard curve were serially diluted with kit-provided dilution buffer until the sample concentration was within the working range of the kit. The assay detects all microcystin and nodularin variants with the ADDA side group but does not provide data for specific congeners. Dissolved toxin values were derived by subtracting particulate microcystin concentrations from total microcystin concentrations.

Vertical profiling of water column structure (depth, temperature, dissolved oxygen) was conducted at all ten stations during the boat surveys using an RBR Concerto® (<https://rbr-global.com/>; RBR, Ottawa, ON, Canada). Operation and maintenance of water quality sensors followed the manufacturer’s recommendations.

2.3. Vertical Profiling Using a Wirewalker

A Wirewalker vertical profiler [26] was moored at Station 4 (S4&WW) in Figure 1A, at 39°1.767', 122°46.092') in 2020 for nearly the entire month of August (Figure 1A–C). The Wirewalker is a profiling platform that uses wave energy to gain downward motion of a positively buoyant instrument along a moored wire. The instrument ratchets down the wire to a fixed depth (approximately 1–2 m from the lake bottom) at which point a trigger releases it from the ratcheting mechanism to allow it to float up the wire to the surface, where it reengages the ratchet. The Wirewalker during this study was equipped with an RBR Concerto® that simultaneously measured depth, temperature, dissolved oxygen, and chlorophyll *a* fluorescence. The Wirewalker cycled between depths of 0.3 and 5.2 m, and the RBR Concerto sampled at a rate of 2 Hz. Data were collected from 3 August until 28 August, with a total of 17,777 profiles collected. Figures were generated using R v2024.12.1.

3. Results

Microscopical observations of water samples collected during the boat surveys revealed that the cyanobacterial community of Clear Lake was dominated by *Lyngbya* spp. (Figure 2A,E) during most of August 2020, although several other potentially toxigenic taxa were also observed throughout the month. *Gloeotrichia* spp. (Figure 2D) was observed during the first week of observation, particularly at Stations 4 and 7 near the confluence of the three Arms of the lake, while *Microcystis* spp. (Figure 1B–D) was also common throughout August, particularly at stations within the Lower and Oaks Arms. *Dolichospermum* spp. was a common sub-dominant genus throughout the lake during the study (Figure 2F). More detailed information on the cyanobacterial community composition during this study and additional dates have been reported by Kalra et al. [5].

3.1. Lakewide Observations 2020

AUV missions revealed the highly heterogeneous nature of chemical and biological parameters in Clear Lake during the period 5–7 August 2020 (Figure 3). Overall, temperature along the main axes of the three Arms of the lake was warmer at their eastern ends, and temperature gradients horizontally were generally greater than gradients vertically in each Arm (Figure 3A).

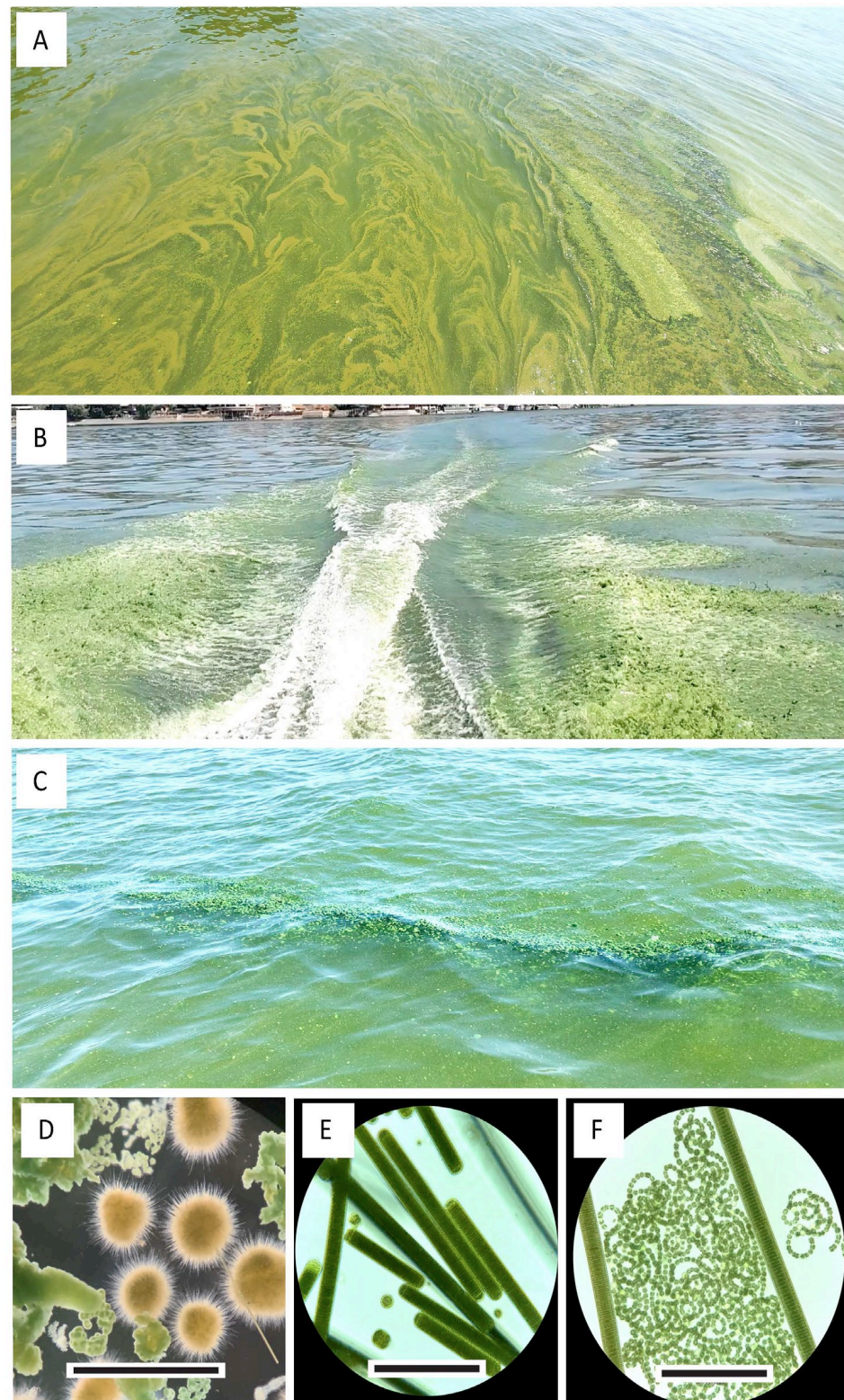


Figure 2. Surface manifestations of cyanobacterial taxa in Clear Lake (A–C), and light micrographs of dominant genera (D–F). Surface scum during a *Lyngbya* bloom (A) and a photomicrograph showing its large filaments (E). Surface accumulations (B,C) dominated by *Microcystis* showing ‘paint-like’ scum (B) and discrete ‘clumps’ (C). A photomicrograph of *Microcystis* colonies (green lumps) and several large *Gleotrichia* colonies (yellow-brown) displaying radially arranged filaments (D). Photomicrograph of *Dolichospermum* colonies (F) bounded by two larger filaments of *Lyngbya*. Marker bars are 200 μm (D) and 20 μm (E,F).

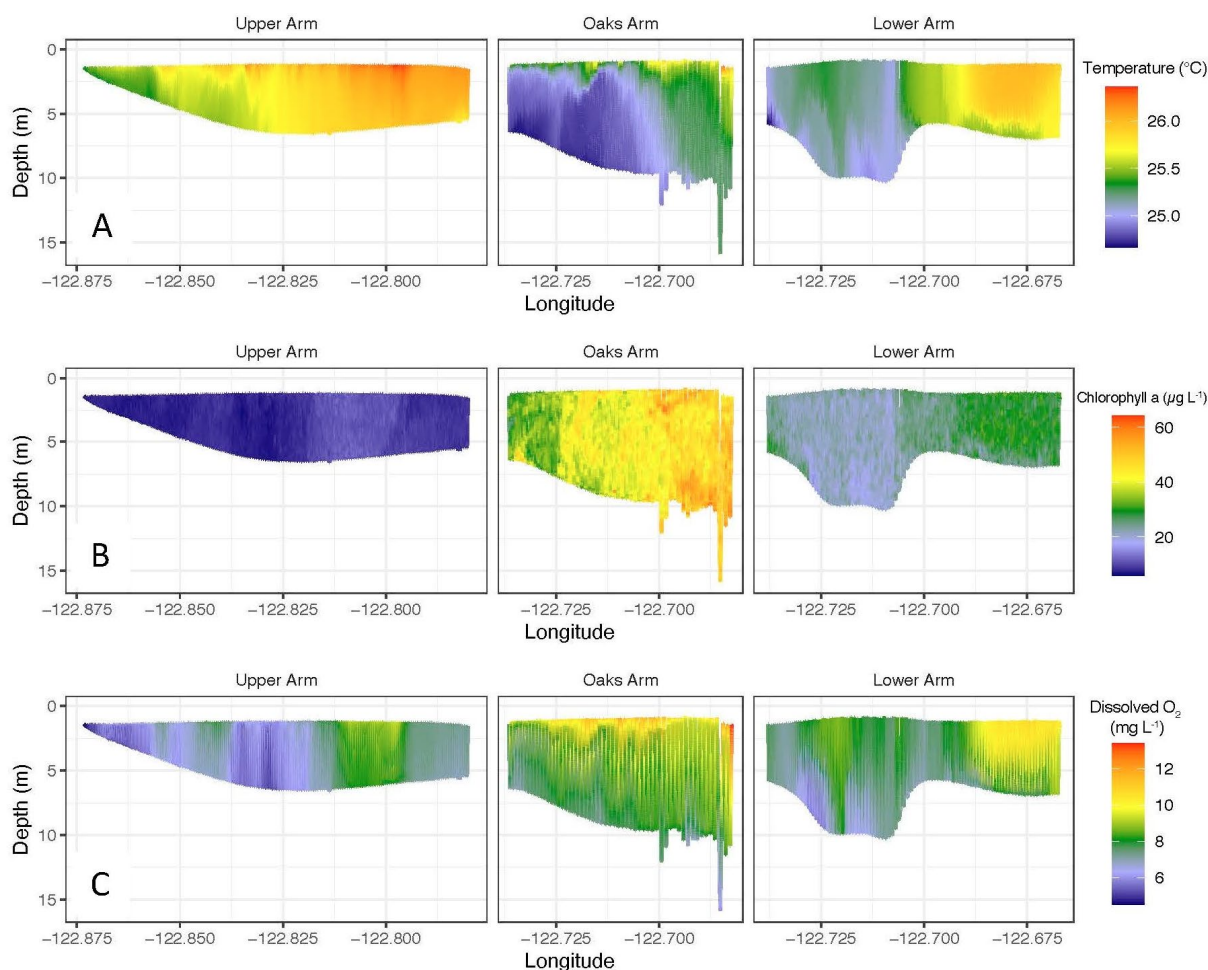


Figure 3. Horizontal-vertical profiles of chemical/physical parameters collected using the Xylem i3XO EcoMapper along the major axes of the three Arms of Clear Lake, August 2020. Profiles of sensed parameters have been contoured and are depicted in columns arranged left to right, respectively, for the Upper, Oaks, and Lower Arms of the lake. Sensed parameters are temperature (A), chlorophyll-*a* fluorescence (B), and dissolved oxygen concentrations (C).

Weak vertical stratification of temperature, limited primarily to very-near surface depths, was apparent in Upper and Oaks Arms, although temperature in the Lower Arm was nearly isothermal vertically at any given location (Figure 3A top right panel), implying relatively complete vertical mixing at that time (7 August). Water temperature in Oaks Arm on 6 August exhibited a pronounced lateral gradient of temperature along the axis of the Arm. This pattern was presumably a result of wind-driven circulation driving warmer surface waters towards the eastern end of the basin and subducting them to greater depth. The presence of warm water near the bottom of Oaks Arm on 6 August may also be due in part to the presence of thermal vents at the bottom of the Arm. Note that the approximately top 2 m of the water is not depicted in the AUV profiles because the AUV was programmed not to enter that layer in order to avoid boat strikes.

Chlorophyll fluorescence was markedly lower in the Upper Arm relative to concentrations observed in the Oaks or Lower Arms at the time of AUV deployments, indicating a much lower standing stock of algal/cyanobacterial biomass in the Upper Arm relative to the other Arms at the time of the survey (values generally $\leq 10 \mu\text{g/L}$ in Figure 3B). In contrast, chlorophyll fluorescence was observed at concentrations $> 30 \mu\text{g/L}$ in the Oaks Arm. Similarly to the pattern observed for temperature, chlorophyll fluorescence in Oaks Arm revealed a strong lateral gradient (concentrations increasing west to east) rather than

a vertical gradient, further implicating wind-driven west-to-east transport and subduction of water near the eastern end of Oaks Arm and to greater depths (carrying attendant algal/cyanobacterial biomass with it). Massive surface accumulations of cyanobacteria were occasionally visible by eye in the Oaks Arms at the time of the AUV deployment. Lower Arm exhibited intermediate concentrations of chlorophyll fluorescence relative to the other two Arms, with greater concentrations observed at the eastern end of Lower Arm.

The horizontal distribution of dissolved oxygen concentrations in the lake generally followed the pattern observed for chlorophyll fluorescence, although differences in concentrations were somewhat muted compared to differences in algal/cyanobacterial biomass. Lower overall concentrations were observed in the Upper relative to the Oaks and Lower Arms (Figure 3C). Dissolved oxygen concentrations were lowest at the eastern ends of Upper and Lower Arms. Vertical stratification in dissolved oxygen concentrations was apparent in Oaks Arm, and to a lesser extent in Lower Arm. These vertical gradients did not completely mirror vertical gradients in chlorophyll fluorescence and were presumably due to rapid oxygen utilization in deeper waters of the Arms.

3.2. Discrete Water Samples and Vertical Profiles During Boat Surveys

Boat surveys conducted on eight dates throughout August (see Materials and Methods) revealed substantive and often rapid changes in water column structure, indicating highly dynamic water column processes (Figures 4 and 5). Overall, surface water temperatures ranged between 24.9 °C and 29.4 °C. Vertical temperature profiles of the water column were generally more similar at all stations throughout the lake on a given day than they were at any single station across all days in the month (rows or columns, respectively, in Figure 4). For example, most water columns were nearly isothermal on 5 August, while pronounced thermoclines were apparent at all stations on 14 August, and the water columns at all stations were nearly isothermal again on 25 August. The pattern gleaned from the collective dataset indicates a rapidly evolving, wind-dominated situation with respect to water column structure.

Vertical patterns of dissolved oxygen concentrations in the water column of Clear Lake during August 2020, obtained with the handheld instrument, also exhibited substantial heterogeneity in percent saturation in both time and space (Figure 5). Oxygen saturation ranged between 71% and 220% in surface waters, with generally lower values occurring at depth. Few generalities with respect to these patterns were apparent, other than that periods and locations exhibiting well-mixed water columns (Figure 4) tended to exhibit relatively similar concentrations of dissolved oxygen throughout the water column, as one might anticipate (compare dates/stations in Figure 4 with corresponding panels in Figure 5). Conversely, stations and dates with well-stratified water columns tended to exhibit large changes in dissolved oxygen with depth. Very low or undetectable dissolved oxygen concentrations were present at or near the bottom of the water column at many stations and dates (Figure 5). Supersaturation of dissolved oxygen was notable at the surface at some stations on some dates (e.g., stations 9 and 10 on 14 August). Even in those instances, however, dissolved oxygen near the lake bottom was often near or at 0% saturation.

Extracted chlorophyll concentrations (a proxy for total phytoplankton biomass) in near-surface water samples collected at each station during the boat surveys exhibited a bimodal temporal distribution during August 2020 (Figure 6A). Stations in the Upper Arm exhibited the lowest values of chlorophyll concentration early in the month, consistent with the profiles obtained using the AUV (Figure 3). Chlorophyll concentrations in the Oaks and Lower Arms were relatively high in early August (averages on 8 August for stations in those Arms were 80 and 108 µg/L for the Oaks and Lower Arm, respectively), followed by minimal values (but still substantial; >20 and 40 µg/L) on 14 August. Chlorophyll

in all Arms increased gradually after 14 August through the end of the month to values averaging 76–88 $\mu\text{g/L}$ for all stations in each Arm (constituting blooms as defined by a target chlorophyll-*a* concentration of 73 $\mu\text{g/L}$ established in the 2007 TMDL [13]). A total of 18% of samples collected during August were greater than that concentration, with most of the 18% observed in the Oaks Arms (Figure 6A). Extracted chlorophyll concentrations in the samples collected during the boat surveys on 5 and 8 August were generally in agreement with chlorophyll fluorescence values obtained using the AUV on 5–7 August in that Oaks and Lower Arms exhibited higher chlorophyll fluorescence than Upper Arm (compare Figures 3B with 6A). However, spatial and temporal heterogeneity observed using the AUV were more pronounced than in the discrete samples (Figures 3B and 6A).

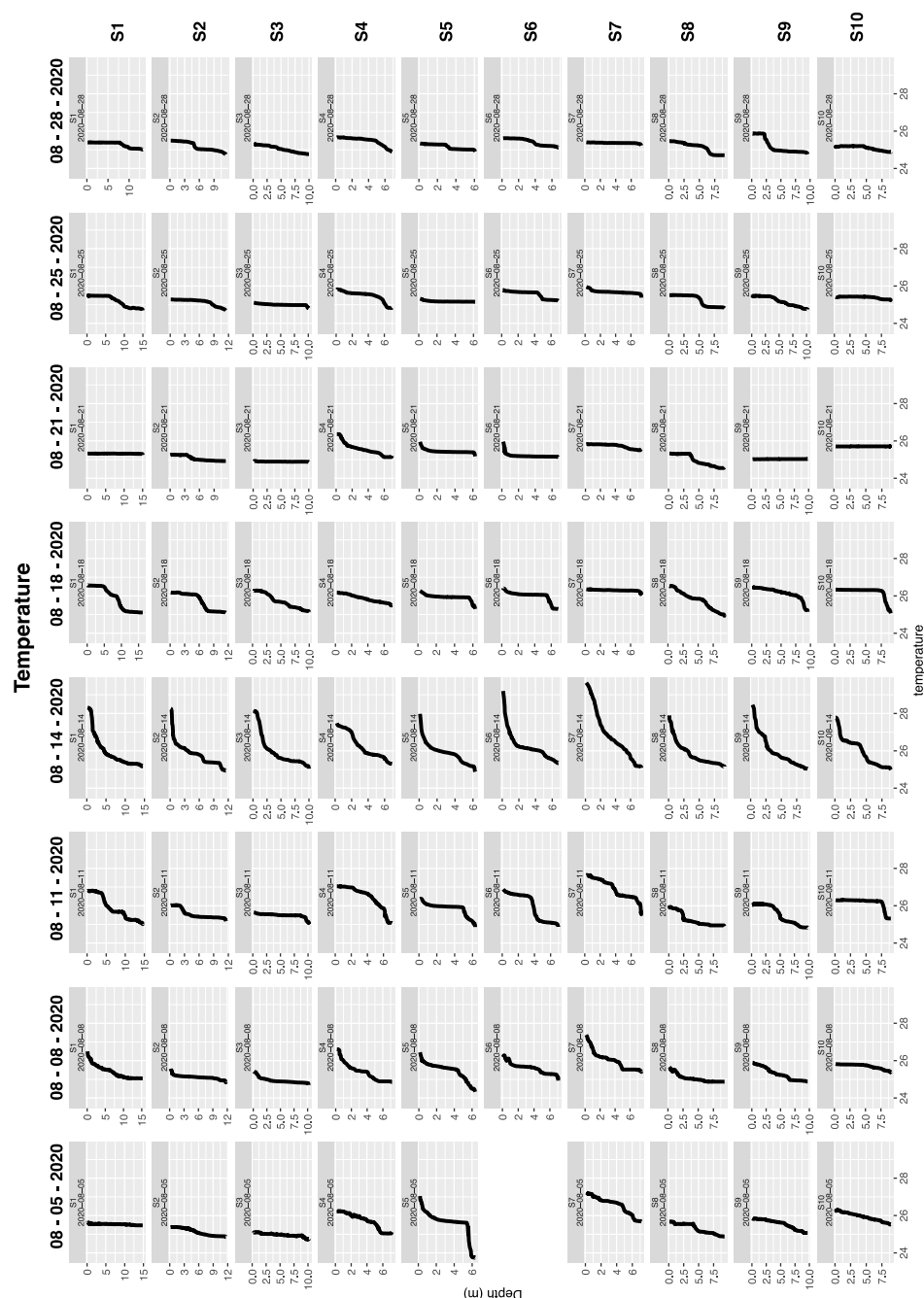


Figure 4. Vertical profiles of water column temperature collected at ten locations throughout Clear Lake on eight sampling dates in August 2020. One missing value on 5 August was due to an instrument malfunction.

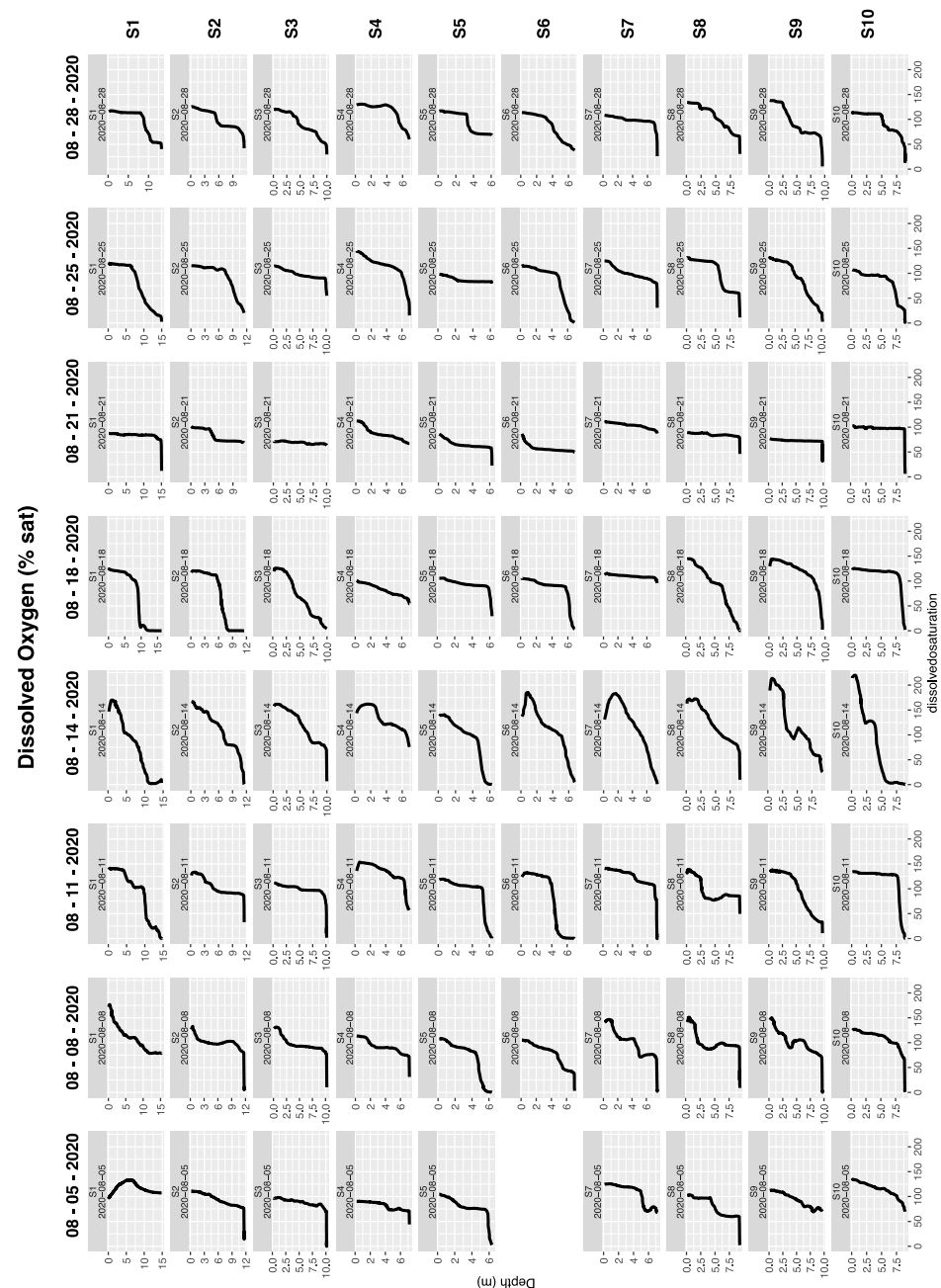


Figure 5. Vertical profiles of water column dissolved oxygen concentrations collected at ten locations throughout Clear Lake on eight sampling dates in August 2020. One missing value on 5 August was due to an instrument malfunction.

All ten sampling stations were positive for total microcystins at least once during the month of August 2020, although concentrations were heterogeneous spatially and temporally (Figure 6B). Temporally, total microcystin concentrations in the discrete water samples were highest on the first two sampling dates in early August, particularly in the Lower Arm. The highest concentration of total microcystins observed was 5.08 $\mu\text{g/L}$, which occurred at station 8 on 8 August. The highest values observed at several other stations also occurred on 8 August, although at lower concentrations than observed in Lower Arm at station 8. Following 8 August, lower concentrations of total microcystins were observed at all sampling locations in the lake, although cyanotoxin was still detected at most stations, particularly in the Lower Arm (Figure 6B). All ten stations were positive for total microcystins on the last sampling date (28 August), albeit at modest concentrations at most

stations. Overall, the California cautionary guidance level for microcystins in recreational waters ($0.8 \mu\text{g/L}$) was exceeded a total of 19 out of 80 times during the month of August, all of which occurred in the Lower and Oaks Arms of the lake (Supplemental Figure S1). The Upper Arm of the lake was consistently lower in microcystin concentrations than the Oaks and Lower Arms (Figure 6B, Supplemental Figure S1).

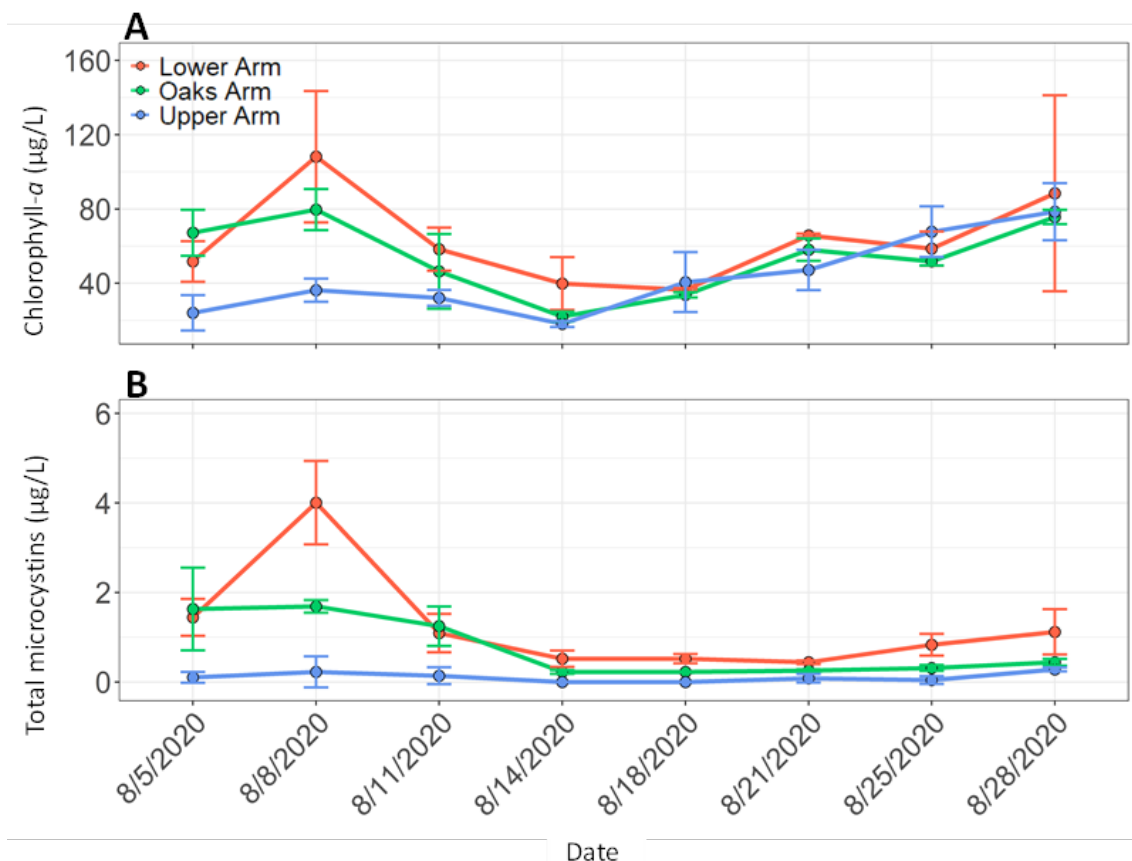


Figure 6. Concentrations of extracted chlorophyll-*a* (A) and microcystins (B) in near-surface water samples collected at ten locations throughout Clear Lake on eight sampling dates in August 2020, averaged by major Arm of the lake (Upper, Oaks, and Lower Arms).

The partitioning of microcystins between the particulate and dissolved pools varied across stations and time (Supplemental Table S2). At most stations, the concentration of cyanotoxins in the particulate pool comprised the smaller fraction of the total toxin pool, with the overall percentage of detectable toxin present in the dissolved fraction ranging from 73 to 97% of the total.

In contrast to chlorophyll fluorescence and cyanotoxin concentrations, concentrations of total nitrogen (TN) and total phosphorus (TP) in near-surface water samples collected during the boat surveys displayed relatively little variation among sampling locations or sampling dates within each Arm of the lake (Figure 7). Interestingly, and somewhat surprisingly, average TP concentrations were generally highest at the Upper Arm stations and lowest at the Lower Arm stations on any given sampling date, with values in Oaks Arm intermediate to the other Arms (Figure 7B). These findings were the inverse of patterns observed for chlorophyll fluorescence and microcystin concentrations (Figure 6). TN concentrations exhibited only minor variations over space (station locations and Arms of the lake; Figure 7A) and time (sampling date), and TN:TP ratios were low for all dates and locations (range for 79 measurements = 0.5–2.2 by atoms).

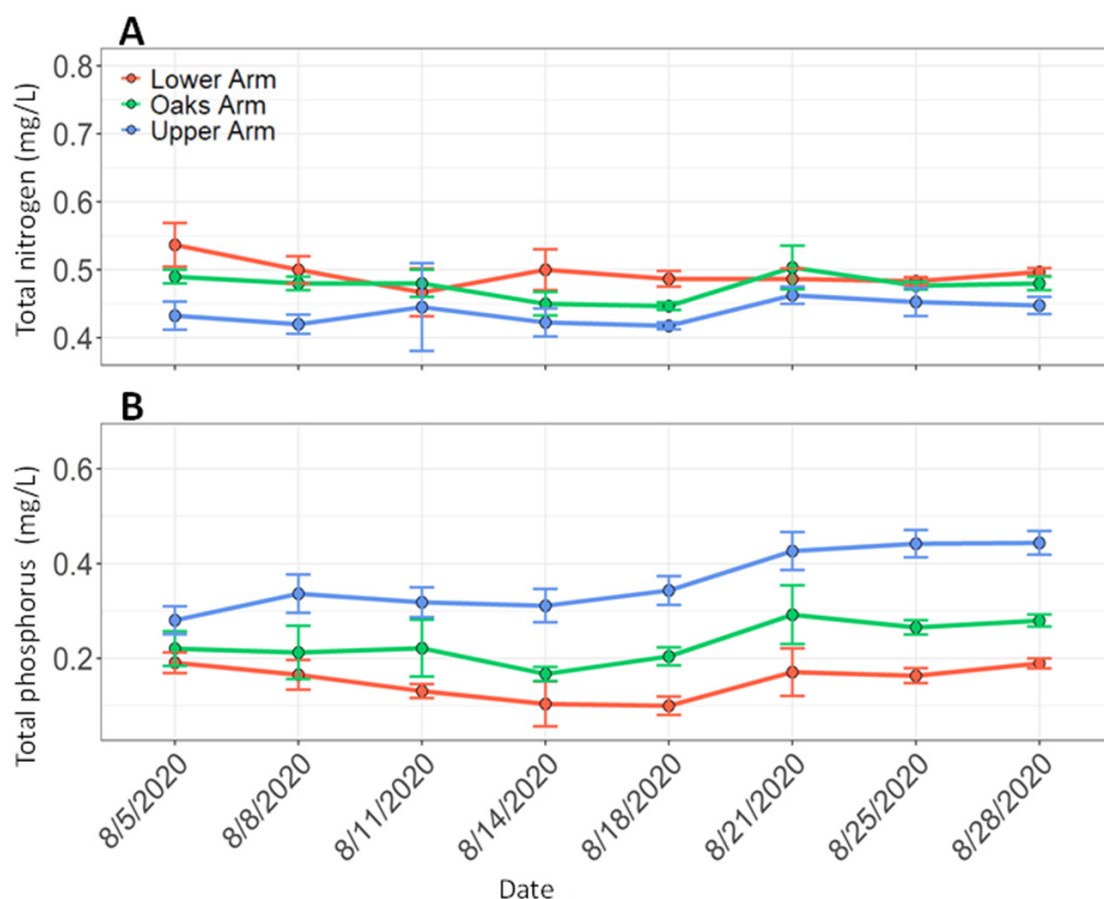


Figure 7. Concentrations of total nitrogen (A) and total phosphorus (B) in near-surface water samples collected at ten locations throughout Clear Lake on eight sampling dates in August 2020, averaged by major Arm of the lake (Upper, Oaks, and Lower Arms).

3.3. Water Column Structure Evolved Rapidly at a Mid-Lake Station

Sensor data collected using the Wirewalker in August 2020 provided high-resolution temporal data encompassing thousands of sensed values across multiple chemical/physical parameters collected throughout the nearly month-long deployment (Figure 8). Additionally, wind speed and direction were collected from a meteorological station (Figure 8A). Wind direction is shown by the orientation of each vector along a line of time, while wind speed is depicted as the length of each vector. Wind direction was predominantly north-westerly during August 2020 (the typical wind direction on the lake; see circular summary of wind direction and magnitude on the insert for Figure 8A), but short periods of wind reversal occurred (especially noticeable as upward-pointing vectors during mid-August and twice near the end of August). Periods of calm winds were also observed, but are difficult to visualize in Figure 8A because they are displayed as vectors of zero magnitude.

A few general trends in temperature, chlorophyll, and dissolved oxygen were apparent across the near-month-long deployment of the Wirewalker at the resolution of the information presented in Figure 8 (Figure 8B–E). The onboard sensors recorded data continuously as the Wirewalker descended and rose. Therefore, the values for each parameter indicate the range observed between the shallowest and deepest depths (0.3 to 5.2 m) for each vertical excursion. For example, the descent and rise in the instrument throughout its deployment resulted in near-constant changes in depth, yielding a tightly packed series of depth excursions (Figure 8B). Periods of calm winds (i.e., waves insufficient to propel the instrument down the wire) are shown as narrow white ‘gaps’ in the overall pattern.

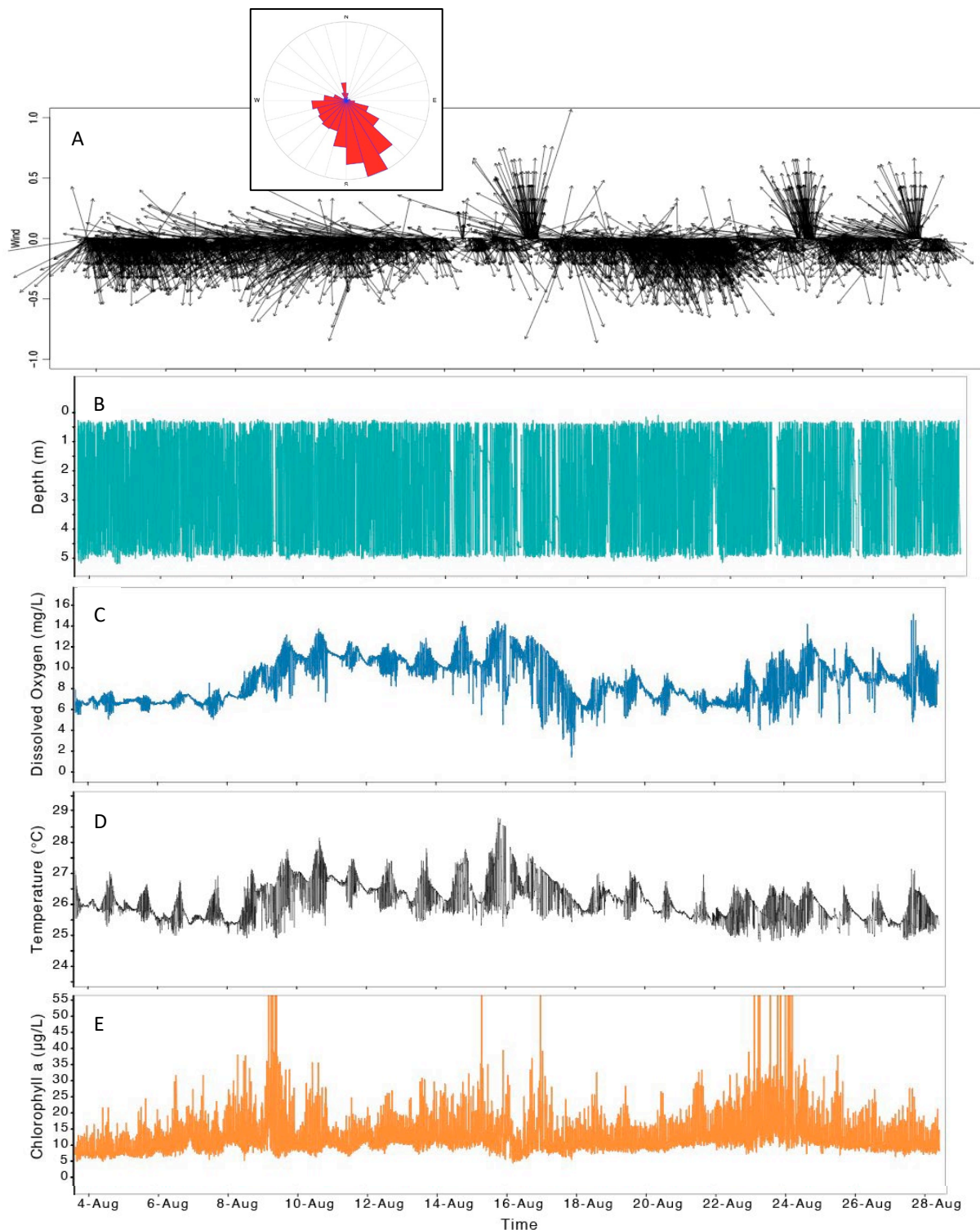


Figure 8. Summary of wind speed (A) and direction (inset in A) obtained from a NOAA CIMIS station closest to Clear Lake, and sensed data collected using the instrumented Wirewalker profiler. The sensed measurements include all data collected during the 25-day deployment in August 2020 in Clear Lake for the instantaneous depth of the sensor package (B), dissolved oxygen concentration (C), temperature (D), and chlorophyll *a* fluorescence (E). Ranges for the values of dissolved oxygen, temperature, and chlorophyll *a* fluorescence indicate the changes in those parameters as the instrument moved down and up on the wire. The nearly solid teal color for depth (B) indicates that the instrument was moving almost continually during the deployment, with occasional pauses in vertical movement (shown by white areas) when wave action at the surface was insufficient to incrementally ratchet the instrument package down the wire (see text for explanation).

The range of temperatures observed throughout the water column was smaller during the period 4–9 August than for other periods, with greater ranges observed 14–18 August, while ranges were more constrained again through the end of the deployment. The pattern reflects the general warming of the water during August, but it also reflects the vertical movement of water in the water column. Mixing would tend to minimize temperature differences between shallow and deep water (i.e., yield narrower ranges of temperature). Water column profiling conducted at station 4 (near the Wirewalker) using the handheld sensor package during the boat surveys tended to support this supposition. Warming surface waters were apparent in temperature profiles between early August and approximately 14 August, with generally more well-mixed water columns from that date until the end of the study (station 4 in Figure 4). The largest temperature range observed during August occurred on 16 August (Figure 8D), indicating the greatest water stratification at that time, just prior to a mixing event recorded by the handheld profiles at station 4 (18 August in Figure 4).

Also obvious from the month-long dataset obtained using the Wirewalker is that the ranges of dissolved oxygen concentrations observed in the water column were greatest for the period 14–17 August (Figure 8C), the same time period when water column stability was greatest (i.e. temperature ranges were greatest; Figure 8D, and station 4 in Figure 4). The most plausible explanation for the large range of dissolved oxygens in the water column at that time is that periods of calm winds (and therefore greater water column stability) resulted in the rapid utilization of dissolved oxygen, presumably at depth and/or at the sediment surface, while high oxygen concentrations in near-surface waters were maintained via photosynthetic production and/or exchange with the atmosphere.

The pattern of chlorophyll fluorescence throughout August revealed relatively few general trends other than that extremely high values tended to occur during periods of greatest water column stability (compare large excursions in water column temperature in Figure 8D with the highest chlorophyll values in Figure 8E). Since the appearance of the highest values occurred on time scales that could not be explained by cell growth, and often occurred at depth, they presumably indicate the sinking and accumulation of algae and/or cyanobacteria near the bottom of the lake (see below).

Periods of calm winds in the month-long deployment of the Wirewalker were apparent as small white areas in the panel of depth of the instrument versus time (Figure 8B). Closely packed teal lines indicate the vertical position of the instrument as it moved continuously up and down the mooring wire. However, the Wirewalker moved down the wire only when wave action was sufficient to engage the internal ratchet mechanism. When wave action was insufficient, the instrument ‘paused’ at a particular depth (but continued sensor measurements) until wave action was again sufficient to activate the ratchet (i.e., depth of the instrument remained constant during calm winds). This situation provided an extremely useful time stamp of periods when winds were very light or calm. Periods of quiescent winds, in turn, provided insight into changes in water column chemistry that accompanied calm conditions.

Examining the Wirewalker dataset at higher temporal resolution during an approximately three-day period in mid-August provided insight into the short-term (days) dynamics and response of water-column chemistry in the lake during periods of calm (Figure 9). In particular, dissolved oxygen concentrations during the period 15 August to 18 August were relatively high (in some cases supersaturated) in the upper water column, with replete conditions near the bottom of the instrument’s vertical excursion (Figure 9 on 15 August at 12:00 h, and 16 August at 12:00 h). During the evening of those days, however, the Wirewalker ‘paused’ in the water column due to reduced wave action.

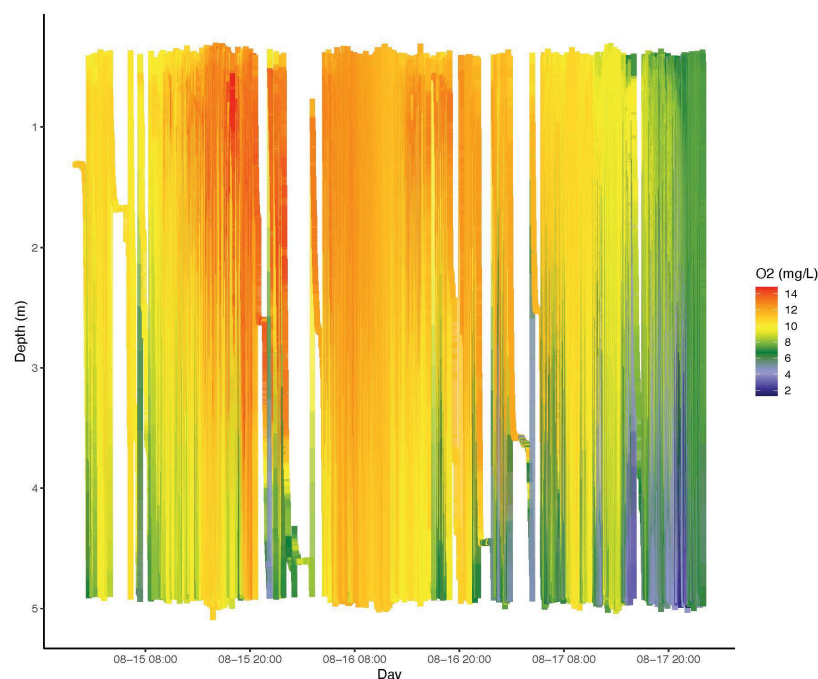


Figure 9. Time-averaged dissolved oxygen concentrations collected by the instrumented Wirewalker profiler in Clear Lake over an approximately three-day period, 15–18 August (a component of the month-long deployment shown in Figure 8). Note the low dissolved oxygen concentrations observed episodically near the bottom of the instrument profiles, especially at the time or following pauses in the vertical movement of the instrument (indicating quiescent wind/wave conditions at the lake).

Upon renewed vertical movement of the instrument package, markedly lower dissolved oxygen concentrations were observed in the deeper waters (deep blue color in Figure 9). These low concentrations represent a rapid onset of hypoxic conditions near the bottom of the lake, presumably due to microbial metabolism at and near the sediment surface during reduced vertical water movement during calm winds. Higher wind and wave action on these two days (as indicated by the renewed movement of the instrument package) resulted in effective reoxygenation of deep water observed in subsequent vertical profiles. However, the hypoxic conditions established on 17 August persisted, and lower dissolved oxygen concentrations were observed in the entire water column at that time. Interestingly, these minima in deep water dissolved oxygen concentrations corresponded to late night, perhaps indicating a diel rhythm in dissolved oxygen concentrations in deep water of the lake that was in synchrony with diel changes in wind forcing. A much more highly resolved (i.e., higher temporal resolution) revealed the detailed sensor data afforded by the use of the Wirewalker (Supplemental Figure S2).

4. Discussion

A difficult task faced by researchers and water managers studying Clear Lake is the sheer size of the lake, further complicated by the complex structure of the basin and the interplay between the three Arms of the lake. Limited resources and personnel have made it difficult to obtain a synoptic, lakewide characterization of its chemistry, physics, and biology, and at the same time gain information on the spatial and temporal heterogeneity across its expanse.

4.1. Complementary Information for Lakewide Assessment from AUV Missions and Boat Surveys

Near-synoptic measurements of temperature, chlorophyll, and dissolved oxygen using the Xylem YSI i3XO EcoMapper provided unprecedented insight into the spatial

heterogeneity that characterizes the lake, and the relatively distinct physics and chemistry of the three Arms during August 2020 (Figure 3). One obvious finding arising from the AUV missions was the more oligotrophic nature of Upper Arm relative to the other Arms of the lake (Figure 3B). This distinction, and the tendency for massive accumulations of algal/cyanobacterial biomass and high cyanotoxin concentrations at the eastern and southeastern ends of the lake (Oaks and Lower Arms), has been well-established from extensive boat and land-based monitoring efforts that have been conducted for more than a decade in Clear Lake (<https://www.bvrancheria.com/clearlakecyanotoxins>; URL accessed on 10 July 2025). These efforts have routinely documented much higher phytoplankton biomass and cyanotoxin concentrations in nearshore samples collected in the eastern Arms of the lake relative to those parameters in the Upper Arm.

Moreover, near-synoptic, detailed temperature profiles of the three Arms obtained using the AUV indicated much stronger horizontal gradients compared to vertical gradients at the time of the deployments. In particular, Oaks and Lower Arms exhibited very strong horizontal gradients, rather than distinct vertical gradients of temperature (Figure 3A). Oaks Arm exhibited a pattern that implied downwelling at the eastern end of the lake, resulting in the subduction into deeper waters of some of the high phytoplankton biomass present at that time (Figure 3B). This pattern is in general agreement with the results of models predicting the circulation pattern in the Oaks Arm [16], which noted the potential for downwelling at the eastern end of the Arm.

Use of the AUV yielded detailed, lakewide, horizontal and vertical profiles on short time frames, much shorter than can be achieved through the collection and analysis of discrete water samples. Additionally, the profiles revealed biologically relevant features of the water column (e.g., water column thermal stratification or downwelling; Figure 3A), information that can be complementary to other large-scale sensing approaches such as satellite imagery. Collectively, these near-synoptic approaches can provide information on spatial heterogeneity that is highly relevant to programs monitoring water quality. For example, Sharp et al. [27] employed a multi-instrument approach in Clear Lake to determine the spatial scale critical to designing cHAB sampling programs [28]. The authors concluded that critical scales of variability in Clear Lake were 70–170 m. Sampling at broader spatial scales may miss important features, information that should be taken into account when designing and conducting cHAB sampling. Thus, in combination with satellite imagery that can provide near-surface spatial and temporal bloom dynamics [29], detailed vertical information provided by AUVs can provide lakewide depictions that can be used to identify possible ‘worst case scenarios’ for cHABs within the lake (e.g., locations with high algal/cyanobacterial biomass that warrant further measurements and/or the collection of discrete samples). The efficient use of limited resources available for sampling and analysis is a fundamental consideration in cHAB monitoring programs.

Lakewide monitoring is also critical for evaluating the response of lakes to management practices imposed to improve water quality. For large, dynamic lakes such as Clear Lake, remote and automated sensing can be instrumental in establishing overall lake status, while dependence on discrete sample monitoring by itself may be insufficient for accurately assessing changes in a lake [30]. This supposition is supported by the highly ephemeral nature of potentially important hydrological events such as the near-bottom hypoxia observed in the present study (Figure 9).

AUV use can also be less labor-intensive than in-person monitoring programs because waypoint deployments and retrievals require no direct observation during the missions. However, instrument cost is significant, and the AUV employed in the present study was not equipped for sample collection along the transects. While onboard, automated sampling is possible with some larger AUVs [21], such instruments are not generally practical or

affordable for most freshwater surveys. Moreover, relatively poor correlations between chlorophyll fluorescence and the presence and concentrations of cyanotoxins [8] make the use of remotely sensed phytoplankton biomass a poor indicator of the toxin status of many waterbodies, including Clear Lake. Discrete water sampling remains the only means of obtaining such information.

As a consequence, the boat surveys conducted as a part of this study provided complementary data on water column structure (temperature, dissolved oxygen) at specific locations throughout the lake, as well as water sampling for the determination of nutrient, chlorophyll-*a* and cyanotoxin concentrations in near-surface water samples at each station (Figures 4–7). At present, cyanotoxins (a focal issue in cHAB monitoring) can only be determined from water samples analyzed in the laboratory. Discrete water samples, therefore, played an important role in the overall characterization of the chemical, physical, and biological status of Clear Lake in August 2020.

Chlorophyll and cyanotoxin concentrations obtained from the discrete water samples provided quantitative information on the distribution of cHAB-related features of the lake. These two parameters, averaged by Arm of the lake for each sampling date, correlated reasonably well in the present study (Figure 6). A moderate correlation between microcystins and chlorophyll concentrations has been previously reported for Clear Lake using a much larger dataset [8]. Locations exhibiting high phytoplankton biomass detected by synoptic remote sensing approaches may therefore provide guidance on where to sample for cyanotoxin presence [31]. In contrast, TN and TP exhibited relatively minor differences temporally or spatially during the present study and provided little interpretive power on the location or magnitude of blooms, or concentrations of cyanotoxins, although low TN:TP ratios implied a nitrogen-limited plankton community at the time of the study.

4.2. High-Resolution Sensing Provided Unprecedented Insight into Water Column Dynamics

High-resolution temporal sensing in the water column of Clear Lake during August 2020 provided unique insight into the temporal dynamics of water chemistry that may contribute directly to the stimulation or maintenance of cHABs. Wirewalker measurements in this study recorded periods when wave action was insufficient to move the instrument package down the mooring wire (Figures 8 and 9, Supplemental Figure S2). These periods of relatively calm winds were an important factor contributing to the rapid development of hypoxic/anoxic conditions in deep water at or near the sediment surface, responses that were apparent at the deepest excursions of the instrument immediately following the return of wave action sufficient to move the instrument down the wire (Figure 9).

The development of hypoxic and anoxic conditions in the deep waters of large lakes is often assumed (or documented) to occur over long time scales (often seasonally), with persistence ranging up to months or longer. For example, Bouffard et al. [32] reported long-term temporal records (140 days) of dissolved oxygen profiles in Lake Erie. The records identified long-term trends in hypolimnion anoxia. However, rapid oxygenation/deoxygenation events as a consequence of wind might also be expected in shallow lakes with long fetches. Indeed, our Wirewalker profiles (and vertical profiles obtained during the boat surveys) indicated that water column mixing and stratification evolved rapidly (within hours) in Clear Lake, at least during the summer. The hypereutrophic nature of the lake appears to enable rapid depletion of dissolved oxygen at and near the sediment surface (within hours) once water column mixing diminishes.

Unfortunately, direct measurements performed during our study in Clear Lake in August 2020 did not include highly temporally resolved sampling for total phosphorus or soluble reactive phosphorus. Such information could have made a direct link between phosphorus release from the sediments, hypoxic/anoxic conditions observed intermittently

during our month-long deployment of the Wirewalker, and the role of wind stress during these events. However, a relationship between anoxia and phosphorus release from sediments is well-established [33], and appears to be a common phenomenon contributing to cHABs in other hypereutrophic lakes in California [34], nationally [35] and internationally [36]. The widespread occurrence of deoxygenation of lakes documented among nearly 400 lakes between 1941 and 2017 indicates a strong potential for increases in internal nutrient loading as drivers of cyanobacterial blooms, particularly among warm and eutrophic lakes [37]. Correlations between these conditions and cyanobacterial dominance [38] and toxin occurrence [39] bode ominously given future climate scenarios.

Although temporally resolved measurements of phosphorus were not made in conjunction with the Wirewalker in our study, evidence for a link between hypoxia/anoxia and phosphorus release from the sediments has been made convincingly for Clear Lake in recent field studies and reviews [8,12,14]. De Palma-Dow et al. [14] demonstrated that hypoxic/anoxic conditions were correlated with total phosphorus and soluble reactive phosphorus concentrations in a multi-year analysis of Clear Lake. Similarly, seasonal peaks in phosphorus concentrations (soluble reactive phosphorus and total phosphorus) in Clear Lake in a study that overlapped with the timing of our study have been documented [12]. Phosphorus concentrations in the water column in that study peaked seasonally during summer and early fall when dissolved oxygen concentrations were lowest, a pattern that is consistent with analyses of much longer time series reviewed by Smith et al. [8] and De Palma-Dow et al. [14], indicating that the conditions observed during our study were consistent with the historical behavior of Clear Lake. Moreover, large seasonal internal phosphorus loading events coincided with the general timing of the development of anoxia in the deep water of the lake during the summer and fall [12]), and examination of shorter time scales within these overall seasonal patterns indicated that numerous intermittent periods of hypoxia/anoxia occurred in summer and fall. That is, hypoxic/anoxic events could occur on timescales of days to weeks. Our study extends these previous measurements by demonstrating that even very short time periods (i.e., diel) may be sufficient to affect hypoxia/anoxia in the deep water of Clear Lake and, by extrapolation, internal phosphorus loading in the lake. Indeed, the importance of very short-term hypoxic/anoxic events in the lake is deserving of further study.

Clear Lake appears particularly susceptible to decreased dissolved oxygen concentrations when water-column mixing slows, presumably due to its hypereutrophic state. Richerson et al. reported 30 years ago that diel oscillations in dissolved oxygen occurred in Clear Lake, with decreasing oxygen in deep, cooler water during daytime thermal stratification; a condition lasting days during prolonged periods of calm weather [3]. Rueda et al. [18] noted that water column stability, and presumably dissolved oxygen concentration, responded to meteorology on time scales of days to weeks, whereas an earlier study by the same authors provided evidence of rapidly evolving temperature-depth profiles over a 4-day period [17]. While this response time might be true for basin-scale changes, our study demonstrated that water column stratification and accompanying changes in water chemistry locally near station 4 occurred on much shorter time scales. This is not surprising, given the large surface area and orientation of the long axis of the lake in the direction of the predominant winds (see Figures 1A and 8A). The Osgood Index [40], which provides a metric of the susceptibility of a lake for vertical water mixing based on surface area and depth, has apparently not been reported for Clear Lake. However, the relatively shallow depth of the lake and large surface area would suggest a very low value that makes the lake highly prone to mixing events with relatively minor input of energy.

The relationship between wind stress on Clear Lake and dissolved oxygen concentrations in the deeper water of the lake was examined to investigate our premise that wind

speed and/or direction over very short time scales (i.e., diel) affected hypoxic/anoxic conditions (and thus the release of phosphorus from the sediments and movement into the water column). Meteorological data averaged hourly from the California Irrigation Management Information System (CIMIS) Station 106 Sanel Valley (Lat: 38.982581, Long: −123.08928) during our study period were downloaded to compare directly to dissolved oxygen observed using the Wirewalker. The Wirewalker data were filtered to include only dissolved oxygen data obtained across a depth range of >4 m to the bottom of the instrument's descent, averaged hourly. The relationships of dissolved oxygen to both wind speed and wind direction were examined. Wind direction was transformed into the angular deviation from the long axis of Clear Lake (135°), i.e., a deviation of 0° indicates wind originating from either NW or SE, while the maximum deviation of 90° indicates wind originating from either NE or SW. These directions greatly change the fetch of the wind on the lake and thus the level of wind stress for a given wind velocity.

Cross-correlation function analysis indicated that a lag of 5 h resulted in the highest positive correlation between wind speed and near-bottom dissolved oxygen concentration. That is, dissolved oxygen concentrations in the lower water column increased approximately five hours after wind speed increased. That finding is consistent with the premise that wind stress acts to mix water vertically in the lake, reducing deep water anoxia. Additionally, a lag of 5 h also resulted in the highest negative correlation between wind-direction deviation from the long axis of the lake and dissolved oxygen concentration near the lake bottom. That is, a change in wind direction away from the long axis of the lake reduced wind stress on the lake surface, which in turn resulted in more quiescent conditions in deeper waters of the lake and therefore increased hypoxic conditions. A Spearman's rank correlation performed with 5 h-lagged wind speed or degree deviation from the long axis resulted in statistically significant correlations with mean bottom dissolved oxygen ($\rho = 0.12$ and -0.14 , respectively, $p < 0.001$, $n = 574$). These relationships demonstrate the impact of wind on dissolved oxygen concentrations over very short time scales in Clear Lake, which presumably alters the flux of phosphorus out of the sediments of Clear Lake into the overlying water column.

One could speculate that short (diel) hypoxic/anoxic events might not be sufficient to stimulate a massive bloom, but these brief events might release sufficient nutrients from highly organic sediments to initiate a bloom or maintain an existing one. Anderson et al. [41] employed continuous in situ dissolved oxygen and soluble reactive phosphorus (SRP) sensors in Lake Erie to correlate the development of anoxic conditions near the bottom of the lake to the release of SRP from the sediments. The authors noted that the lag time between the development of anoxia and increases in SRP in the overlying waters was short (12–42 h).

These observations imply that repeated 'pulsed' releases of phosphorus from the sediments of Clear Lake during short-term hypoxic/anoxic events observed in this study could constitute significant contributions to the nutrient pools supporting cHABs in the lake. Such intermittent injections of nutrients into the water column might also provide an explanation for the long-lived blooms that typify Clear Lake.

Parenthetically, dissolved oxygen concentration has been reported as the most important environmental parameter controlling the distribution of the hitch, an imperiled minnow endemic to Clear Lake [42]. The effect of the ephemeral hypoxic events observed in this study on fish populations of the lake is unknown.

4.3. Multiple Roles of Wind as a Factor Affecting cHABs in Clear Lake

Modeling the effect of wind on phytoplankton blooms has typically focused on the impact of major wind events (i.e., storms) on water mixing and nutrient intrusions into

lighted waters, and concomitant responses of the phytoplankton community [43]. However, wind forcing can act positively or negatively towards lake ecology and cyanobacterial biology in particular. Strong wind events are well-characterized factors that act to transport nutrients from deep water into shallow water, where phytoplankton can acquire and utilize them. Conversely, wind-induced mixing can deepen mixed layers, thereby reducing light available for phytoplankton growth, and directly affect the ability of some cyanobacterial taxa to migrate vertically in the water column [44].

The absence of strong wind forcing can also have mixed effects on lake biology. Calm weather allows water column stratification, retaining phytoplankton near the surface where light is abundant, but water column stratification also interrupts the upward movement of nutrients from deep water. Further complicating matters, microbial metabolism in the absence of wind-induced mixing can lead to deep water hypoxia or anoxia due to microbial decomposition at the sediment-water interface, as demonstrated in the present study, promoting the redox-dependent release of growth-limiting nutrients such as phosphorus into the overlying water.

These multiple roles played by wind in lake biology are not new, as Mesman et al. [43] have provided model simulations and complementary lake measurements to demonstrate that the effect of wind events on phytoplankton can be positive or negative, depending on the intensity of the wind and specific water column features. This important interplay between wind and lake biology differs from the often one-dimensional view of climate change on cHABs, which has stressed warming temperatures as the underlying cause for the global expansion of cyanobacterial blooms [45,46]. Indirect effects of changing climate, such as altered wind speeds, direction, or number of wind events, are often not considered [47].

Wind, however, is a uniquely significant and multifaceted factor for a lake of the size, depth, geographical orientation, and eutrophic state of Clear Lake. Its shallow depth (average depth ≈ 10 m), altitude (405 m), orientation in line with the prevailing wind direction, long fetch (approximately 30 km), and hypereutrophic condition are key factors mediating the impact of wind on its biology. Wind has been shown to have a ‘direct’ and sometimes dramatic effect on the distribution of floating cyanobacterial biomass in eutrophic lakes. Ortiz et al. [48], for example, made extensive measurements of environmental parameters near the surface of shallow, hypereutrophic Swan Lake. As anticipated, wind direction had a major impact on the distribution of a *Microcystis* bloom present in the lake at the time. Wind direction also contributed significantly to horizontal and vertical spatial heterogeneity in *Microcystis* blooms in eutrophic Lake Taihu [44,49]. Similarly, phytoplankton distributions in Clear Lake were strongly affected by the wind direction and fetch, leading to massive accumulations of biomass in the Oaks and Lower Arms of the lake in early August, lessening mid-month, and then reestablishing during late August (Figure 3). Such accumulations were not observed upwind in the Upper Arm of the lake. The tendency for massive accumulations to be relegated to the Oaks and Lower Arms of Clear Lake has been repeatedly observed by routine monitoring of shoreline sampling stations (<https://www.bvrancheria.com/clearlakecyanotoxins>), and is an obvious direct impact of wind on cyanobacterial distributions in the lake.

The ‘indirect’ effects of wind in Clear Lake appear to be more nuanced than those that are directly observable. As detailed above, periods of calm resulted in the rapid development of hypoxic conditions near the sediment surface at the location of the Wirewalker (Figures 8 and 9). Periods of calm winds and hypoxia/anoxia resulting from reduced water column mixing presumably resulted in ‘pulses’ of phosphorus release from the sediments into the overlying waters. Renewed wind- and water-column mixing in this relatively shallow polymictic lake would then make them available for phytoplankton

growth. Additionally, periods of calm winds during our August study, resulting in the rapid reestablishment of water column stratification, may have provided a competitive advantage for buoyant cyanobacteria relative to many eukaryotic algae [50].

It is important to note that nutrients released from the sediment into the deep waters of Clear Lake need not be thoroughly mixed into surface waters in order to become available to phytoplankton. Colonies of *Goleotrichia*, *Microcystis*, and other cyanobacteria are capable of migrating vertically into the hypolimnion in order to acquire nutrients present at higher concentrations than in surface waters [51–53]. Thus, reduced wind forcing, lowered vertical mixing, and the release of phosphorus into the near-bottom waters of Clear Lake may provide an additional competitive advantage to vertically migrating cyanobacteria of the lake.

5. Conclusions

Near-synoptic sensing in Clear Lake, CA, using an autonomous underwater vehicle, documented a highly heterogeneous distribution of cyanobacterial blooms present at the time, both horizontally along the length of the lake and vertically in the water column in all three major Arms of the lake. The lake's chemistry, physics, and biology were strongly impacted by wind due to the unique combination of lake size, depth, elevation, and orientation to the prevailing wind direction. The direct impact of wind was responsible for massive accumulations of surface-associated cyanobacterial colonies throughout the southeastern portions of the lake. Additionally, an indirect effect of wind was demonstrated using a mechanically driven, continuously monitoring water column profiler. The information gathered indicated the potential for an extremely fast response (within hours) of Clear Lake to periods of low or no wind-driven water column mixing. Specifically, the hypereutrophic status of the lake, enhanced by summer water temperatures, resulted in rapid depletion of near-bottom dissolved oxygen concentrations due to microbial decomposition, creating redox conditions at and near the sediment surface that may lead to the release of phosphorus from the sediments. Thus, intermittent periods of wind and calm (and the latter's effect on dissolved oxygen concentrations at and near the sediment surface) may play a pivotal role in bloom initiation or bloom persistence by releasing 'pulses' of remineralized phosphorus into the water column for subsequent uptake by the phytoplankton community.

Supplementary Materials: The following supporting information can be downloaded at: <https://www.mdpi.com/article/10.3390/w17223265/s1>. Supplemental Figure S1. Map of Clear Lake showing the location of sampling stations (A) and the presence of microcystins on four dates during August 2020 (B–E), presented in relation to the California guidance for cyanotoxin concentrations in recreational waters (https://mywaterquality.ca.gov/habs/resources/habs_response.html, accessed on 11 November 2025). Green circles indicate concentrations of microcystins below 'caution' levels, yellow circles indicate concentrations exceeding the 'caution' advisory level (size of circle proportional to concentration). Supplemental Figure S2. Expanded temporal resolution of Wirewalker data showing approximately 2.5 hours of deployment of the instrumented profiler period. Sensing parameters are depicted by various colors. The slow or stalled downward movement of the instrument package between 20:35 and 22:15 indicates that the surface of the lake was relatively quiescent and therefore unable to activate the ratchet that propels the package down the wire. Note the low dissolved oxygen concentrations (blue line) at depth immediately following this period of quiescence, observed when the instrument regained downward movement. Also note the high chlorophyll-*a* concentrations at depth (relative to concentrations near the surface at 22:17). The high biomass at depth may have contributed to rapid oxygen depletion in deep water (noted between 22:00 and 22:17). Supplemental Table S1. Coordinates of sampling stations in Clear Lake, CA during August 2020. Supplemental Table S2. Range of concentrations of total microcystins, particulate microcystins and dissolved microcystins observed at each sampling station during August 2020.

Author Contributions: D.A.C., E.W. and M.D.A.H. conceived and directed the study. Most field operations and laboratory analyses were performed by B.S., A.T. and K.F., with participation by A.A.Y.L., E.W., J.S., I.K., D.A.C., S.A.S., A.L.W. and S.S. performed all operations with the YSI i3XO EcoMapper. D.A.C. wrote the original draft of the manuscript; all authors participated in reviewing and editing the original draft. All authors have read and agreed to the published version of the manuscript.

Funding: Funding for this project was provided by the Central Valley Regional Water Quality Control Board to the Southern California Coastal Water Research Project and the University of Southern California (agreement numbers 19-078-270-03 and 19-003-150).

Data Availability Statement: All data employed in the study are available from the data repository at <https://zenodo.org/> accessed on 11 November 2025.

Acknowledgments: The authors thank Sara Ryan, Karola Kennedy, Angela De Palma-Dow, and Gerid Ollison for assistance and guidance in the field work, and to Jennifer Beatty with help drafting some of the figures, and to Christine Joab, who was instrumental in assisting with the acquisition of funding for the study.

Conflicts of Interest: Author Stephanie A. Smith, Adam L. Willingham and Shawn Sneddon were all employed by Xylem Environmental at the time of the study. The remaining authors declare that the research was conducted in the absence of any commercial or financial relationship that could be construed as a potential conflict of interest.

References

1. Bradbury, J.P. *Diatom Biostratigraphy and the Paleolimnology of Clear Lake, Lake County, California*. *Late Quaternary Climate, Tectonism, Sedimentation in Clear Lake, Northern California Coasts*; Geological Society of America: Boulder, CO, USA, 1988; pp. 97–129.
2. Richerson, P.J.; Suchanek, T.H.; Zierenberg, R.A.; Osleger, D.A.; Heyvaert, A.C.; Slotton, D.G.; Eagles-Smith, C.A.; Vaughn, C.E. Anthropogenic stressors and changes in the clear lake ecosystem as recorded in sediment cores. *Ecol. Appl.* **2008**, *18*, A257–A283. [[CrossRef](#)] [[PubMed](#)]
3. Richerson, P.J.; Suchanek, T.H.; Why, S.J. *The Causes and Control of Algal Blooms in Clear Lake, in Clean Lake Diagnostic/Feasibility Study for Clear Lake, California*; University of California at Davis: Davis, CA, USA, 1994; p. 182.
4. Borrelli, J.J.; Relyea, R.A. A review of spatial structure of freshwater food webs: Issues and opportunities modeling within-lake meta-ecosystems. *Limnol. Oceanogr.* **2022**, *67*, 1746–1759. [[CrossRef](#)]
5. Kalra, I.; Stewart Brittany, P.; Florea Kyra, M.; Smith, J.; Webb Eric, A.; Caron David, A. Temporal and spatial dynamics of harmful algal bloom-associated microbial communities in eutrophic Clear Lake, California. *Appl. Environ. Microbiol.* **2025**, *91*, e00011–25. [[CrossRef](#)]
6. Goldman, C.R.; Wetzel, R.G. A study of the primary productivity of Clear Lake, Lake County California. *Ecology* **1963**, *44*, 283–294. [[CrossRef](#)]
7. Wrigley, R.C.; Horne, A.J. Remote sensing and lake eutrophication. *Nature* **1974**, *250*, 213–214. [[CrossRef](#)]
8. Smith, J.; Eggleston, E.; Howard, M.D.A.; Ryan, S.; Gichuki, J.; Kennedy, K.; Tyler, A.; Beck, M.; Huie, S.; Caron, D.A. Historic and recent trends of cyanobacterial harmful algal blooms and environmental conditions in Clear Lake, California: A 70-year perspective. *Elementa* **2023**, *11*, 00115. [[CrossRef](#)]
9. Solomon, G.M.; Stanton, B.; Ryan, S.; Little, A.; Carpenter, C.; Paulukonis, S. Notes from the field: Harmful Algal Bloom affecting private drinking water intakes—Clear Lake, California, June–November 2021. *MMWR* **2022**, *71*, 1306–1307. [[CrossRef](#)]
10. Stanton, B.; Little, A.; Miller, L.; Solomon, G.; Ryan, S.; Paulukonis, S.; Cajina, S. Microcystins at the tap: A closer look at unregulated drinking water contaminants. *Water Sci.* **2023**, *5*, e1337. [[CrossRef](#)]
11. Mioni, C.E.; Kudela, R. Harmful cyanobacteria blooms and their toxins in Clear Lake and the Sacramento-San Joaquin Delta (California). *Delta* **2011**, *10*, 058–150.
12. Swann, M.M.; Cortes, A.; Forrest, A.L.; Framsted, N.; Sadro, S.; Schladow, S.G.; De Palma-Dow, A. Internal phosphorus loading alters nutrient limitation and contributes to cyanobacterial blooms in a polymictic lake. *Aquat. Sci.* **2024**, *86*, 46. [[CrossRef](#)]
13. Webber, L. *Amendment to the Water Quality Control Plan for the Sacramento River and San Joaquin River Basins for the Control of Nutrients in Clear Lake*; Staff Report Rancho Cordova, CA; Central Valley Regional Water Quality Control Board: Rancho Cordova, CA, USA, 2006.
14. De Palma-Dow, A.; McCullough, I.M.; Brentrup, J.A. Turning up the heat: Long-term water quality responses to wildfires and climate change in a hypereutrophic lake. *Ecosphere* **2022**, *13*, e4271. [[CrossRef](#)]

15. Small, L.F. Effect of wind on the distribution of chlorophyll *a* in Clear Lake, Iowa. *Limnol. Oceanogr.* **1963**, *8*, 426–432. [[CrossRef](#)]
16. Rueda, F.J.; Schladow, S.G. Dynamics of large polymictic Lake. II: Numerical simulations. *J. Hydraul. Eng.* **2003**, *129*, 92–101.
17. Rueda, F.J.; Schladow, S.G.; Monismith, S.G.; Stacey, M.T. Dynamics of large polymictic lake. I: Field observations. *J. Hydraul. Eng.* **2003**, *129*, 82–91.
18. Rueda, F.J.; Schladow, S.G.; Monismith, S.G.; Stacey, M.T. On the effects of topography on wind and the generation of currents in a large multi-basin lake. *Hydrobiologia* **2005**, *532*, 139–151. [[CrossRef](#)]
19. Rogowski, P.; Terrill, E.; Otero, M.; Hazard, L.; Middleton, W. Mapping ocean outfall plumes and their mixing using autonomous underwater vehicles. *J. Geophys. Res. Ocean.* **2012**, *117*, C07016. [[CrossRef](#)]
20. Seegers, B.N.; Birch, J.M.; Marin, R.; Scholin, C.A.; Caron, D.A.; Seubert, E.L.; Howard, M.D.A.; Robertson, G.L.; Jones, B.H. Subsurface seeding of surface harmful algal blooms observed through the integration of autonomous gliders, moored environmental sample processors, and satellite remote sensing in southern California. *Limnol. Oceanogr.* **2015**, *60*, 754–764. [[CrossRef](#)]
21. Zhang, Y.; Kieft, B.; Hobson, B.W.; Ryan, J.P.; Barone, B.; Preston, C.M.; Roman, B.; Raanan, B.Y.; Marin, I.R.; O'Reilly, T.C.; et al. Autonomous tracking and sampling of the deep chlorophyll maximum layer in an open-ocean eddy by a long-range autonomous underwater vehicle. *IEEE J. Ocean. Eng.* **2020**, *45*, 1308–1321. [[CrossRef](#)]
22. Brenttrup, J.A.; Williamson, C.E.; Colom-Montero, W.; Eckert, W.; de Eyto, E.; Grossart, H.-P.; Huot, Y.; Isles, P.D.F.; Knoll, L.B.; Leach, T.H.; et al. The potential of high-frequency profiling to assess vertical and seasonal patterns of phytoplankton dynamics in lakes: An extension of the Plankton Ecology Group (PEG) model. *Inland Waters* **2016**, *6*, 565–580. [[CrossRef](#)]
23. Marcé, R.; George, G.; Buscarinu, P.; Deidda, M.; Dunalska, J.; de Eyto, E.; Flaim, G.; Grossart, H.-P.; Istvanovics, V.; Lenhardt, M.; et al. Automatic high frequency monitoring for improved lake and reservoir management. *Environ. Sci. Technol.* **2016**, *50*, 10780–10794. [[CrossRef](#)]
24. Minaudo, C.; Odermatt, D.; Bouffard, D.; Rahaghi, A.I.; Lavanchy, S.; Wüest, A. The imprint of primary production on high-frequency profiles of lake optical properties. *Environ. Sci. Technol.* **2021**, *55*, 14234–14244. [[CrossRef](#)]
25. Rogora, M.; Cancellario, T.; Caroni, R.; Kamburska, L.; Manca, D.; Musazzi, S.; Tiberti, R.; Lami, A. High-frequency monitoring through in-situ fluorometric sensors: A supporting tool to long-term ecological research on lakes. *Front. Environ. Sci.* **2023**, *10*, 1058515. [[CrossRef](#)]
26. Pinkel, R.; Goldin, M.A.; Smith, J.A.; Sun, O.M.; Aja, A.A.; Bui, M.N.; Huguen, T. The Wirewalker: A vertically profiling instrument carrier powered by ocean waves. *J. Atmos. Ocean. Technol.* **2011**, *28*, 426–435. [[CrossRef](#)]
27. Sharp, S.L.; Forrest, A.L.; Bouma-Gregson, K.; Jin, Y.; Cortés, A.; Schladow, S.G. Quantifying scales of spatial variability of cyanobacteria in a large, eutrophic lake using multiplatform remote sensing tools. *Front. Environ. Sci.* **2021**, *9*, 612934. [[CrossRef](#)]
28. Blackwell, S.M.; Moline, M.A.; Schaffner, A.; Garrison, T.; Chang, G. Sub-kilometer length scales in coastal waters. *Cont. Shelf Res.* **2008**, *28*, 215–226. [[CrossRef](#)]
29. Hunter, P.D.; Tyler, A.N.; Willby, N.J.; Gilvear, D.J. The spatial dynamics of vertical migration by *Microcystis aeruginosa* in a eutrophic shallow lake: A case study using high spatial resolution time-series airborne remote sensing. *Limnol. Oceanogr.* **2008**, *53*, 2391–2406. [[CrossRef](#)]
30. Davis, T.W.; Stumpf, R.; Bullerjahn, G.S.; McKay, R.M.L.; Chaffin, J.D.; Bridgeman, T.B.; Winslow, C. Science meets policy: A framework for determining impairment designation criteria for large waterbodies affected by cyanobacterial harmful algal blooms. *Harmful Algae* **2019**, *81*, 59–64. [[CrossRef](#)]
31. Stumpf, R.P.; Davis, T.W.; Wynne, T.T.; Graham, J.L.; Loftin, K.A.; Johengen, T.H.; Gossiaux, D.; Palladino, D.; Burtner, A. Challenges for mapping cyanotoxin patterns from remote sensing of cyanobacteria. *Harmful Algae* **2016**, *54*, 160–173. [[CrossRef](#)]
32. Bouffard, D.; Ackerman, J.D.; Boegman, L. Factors affecting the development and dynamics of hypoxia in a large shallow stratified lake: Hourly to seasonal patterns. *Water Resour. Res.* **2013**, *49*, 2380–2394. [[CrossRef](#)]
33. Mortimer, C.H. The exchange of dissolved substances between mud and water in lakes. *J. Ecol.* **1941**, *29*, 280–329. [[CrossRef](#)]
34. Defeo, S.; Beutel, M.W.; Rodal-Morales, N.; Singer, M. Sediment release of nutrients and metals from two contrasting eutrophic California reservoirs under oxic, hypoxic and anoxic conditions. *Front. Water* **2024**, *6*, 1474057. [[CrossRef](#)]
35. Anderson, H.S.; Johengen, T.H.; Miller, R.; Godwin, C.M. Accelerated sediment phosphorus release in Lake Erie's central basin during seasonal anoxia. *Limnol. Oceanogr.* **2021**, *66*, 3582–3595. [[CrossRef](#)]
36. Zhu, G.; Wang, F.; Zhang, Y.; Gao, G.; Qin, B. Hypoxia and its environmental influences in large, shallow, and eutrophic Lake Taihu, China, 1922–2010. *Verhandlungen Des Int. Ver. Limnol.* **2008**, *30*, 361–365.
37. Jane, S.F.; Hansen, G.J.A.; Kraemer, B.M.; Leavitt, P.R.; Mincer, J.L.; North, R.L.; Pilla, R.M.; Stetler, J.T.; Williamson, C.E.; Woolway, R.I.; et al. Widespread deoxygenation of temperate lakes. *Nature* **2021**, *594*, 66–70. [[CrossRef](#)] [[PubMed](#)]
38. Kosten, S.; Huszar, V.L.M.; Bécares, E.; Costa, L.S.; van Donk, E.; Hansson, L.-A.; Jeppesen, E.; Kruk, C.; Lacerot, G.; Mazzeo, N.; et al. Warmer climates boost cyanobacterial dominance in shallow lakes. *Glob. Change Biol.* **2012**, *18*, 118–126. [[CrossRef](#)]

39. Mantzouki, E.; Lüring, M.; Fastner, J.; De Senerpont Domis, L.; Wilk-Woźniak, E.; Koreivienė, J.; Seelen, L.; Teurlincx, S.; Verstijnen, Y.; Krztoń, W.; et al. Temperature effects explain continental scale distribution of cyanobacterial toxins. *Toxins* **2018**, *10*, 156. [\[CrossRef\]](#) [\[PubMed\]](#)
40. Osgood, R.A. *The Limnology, Ecology and Management of Twin Cities Metropolitan Area Lakes*; Metropolitan Council of the Twin Cities Area: St. Paul, MN, USA, 1988.
41. Anderson, H.S.; Johengen, T.H.; Godwin, C.M.; Purcell, H.; Alsip, P.J.; Ruberg, S.A.; Mason, L.A. Continuous in situ nutrient analyzers pinpoint the onset and rate of internal P loading under anoxia in Lake Erie's central basin. *ACS ES&T Water* **2021**, *1*, 774–781. [\[CrossRef\]](#)
42. Feyrer, F.; Young, M.; Patton, O.; Ayers, D. Dissolved oxygen controls summer habitat of Clear Lake Hitch (*Lavinia exilicauda* chi), an imperilled potamodromous cyprinid. *Ecol. Freshw. Fish* **2020**, *29*, 188–196. [\[CrossRef\]](#)
43. Mesman, J.P.; Ayala, A.I.; Goyette, S.; Kasparian, J.; Marcé, R.; Markensten, H.; Stelzer, J.A.; Thayne, M.W.; Thomas, M.K.; Pierson, D.C.; et al. Drivers of phytoplankton responses to summer wind events in a stratified lake: A modeling study. *Limnol. Oceanogr.* **2022**, *67*, 856–873. [\[CrossRef\]](#)
44. Xue, Z.; Zhu, W.; Zhu, Y.; Fan, X.; Chen, H.; Feng, G. Influence of wind and light on the floating and sinking process of *Microcystis*. *Sci. Rep.* **2022**, *12*, 5655. [\[CrossRef\]](#)
45. Paerl, H.W.; Huisman, J. Blooms like it hot. *Science* **2008**, *320*, 57–58. [\[CrossRef\]](#) [\[PubMed\]](#)
46. Paerl, H.W.; Huisman, J. Climate change: A catalyst for global expansion of harmful cyanobacterial blooms. *Environ. Microbiol. Rep.* **2009**, *1*, 27–37. [\[CrossRef\]](#)
47. Nazari-Sharabian, M.; Ahmad, S.; Karakouzian, M. Climate change and eutrophication: A short review. *Eng. Technol. Appl. Sci. Res.* **2019**, *8*, 3668–3672. [\[CrossRef\]](#)
48. Ortiz, D.A.; Wilkinson, G.M. Capturing the spatial variability of algal bloom development in a shallow temperate lake. *Freshw. Biol.* **2021**, *66*, 2064–2075. [\[CrossRef\]](#)
49. Wu, X.; Kong, F.; Chen, Y.; Qian, X.; Zhang, L.; Yu, Y.; Zhang, M.; Xing, P. Horizontal distribution and transport processes of bloom-forming *Microcystis* in a large shallow lake (Taihu, China). *Limnologia* **2010**, *40*, 8–15. [\[CrossRef\]](#)
50. Visser, P.M.; Ibelings, B.W.; Bormans, M.; Huisman, J. Artificial mixing to control cyanobacterial blooms: A review. *Aquat. Ecol.* **2016**, *50*, 423–441. [\[CrossRef\]](#)
51. Istvánovics, V.; Pettersson, K.; Rodrigo, M.A.; Pierson, D.; Padisák, J.; Colom, W. *Gloeotrichia echinulata*, a colonial cyanobacterium with a unique phosphorus uptake and life strategy. *J. Plankton Res.* **1993**, *15*, 531–552. [\[CrossRef\]](#)
52. Barbiero, R.P.; Welch, E.B. Contribution of benthic blue-green algal recruitment to lake populations and phosphorus translocation. *Freshw. Biol.* **1992**, *27*, 249–260. [\[CrossRef\]](#)
53. Overman, C.; Wells, S. Modeling cyanobacteria vertical migration. *Water* **2022**, *14*, 953. [\[CrossRef\]](#)

Disclaimer/Publisher's Note: The statements, opinions and data contained in all publications are solely those of the individual author(s) and contributor(s) and not of MDPI and/or the editor(s). MDPI and/or the editor(s) disclaim responsibility for any injury to people or property resulting from any ideas, methods, instructions or products referred to in the content.